JOURNAL OF GEOPHYSICAL RESEARCH, VOL. 100, NO. A10, PAGES 19,227–19,237, OCTOBER 1, 1995

Simulation study of the Riemann problem associated with the magnetotail reconnection

Y. Lin

Department of Physics, Auburn University, Auburn, Alabama

L. C. Lee

Geophysical Institute and Department of Physics, University of Alaska Fairbanks

Abstract. The structure of reconnection layer in the distant magnetotail is studied by solving the Riemann problem for the evolution of an initial current sheet using one-dimensional MHD and hybrid simulations. Initially, the current sheet with total pressure balance separates the plasmas and fields in the two lobes. In the presence of a nonzero normal magnetic field, which is due to the magnetic reconnection, the initial current sheet evolves to form the reconnection layer, which consists of various MHD discontinuities. First, we study the symmetric case with equal magnetic field strengths, equal plasma densities, and exactly antiparallel magnetic fields (B_y=0) in the two lobes. The Petschek (1964) reconnection layer which contains two switch-off slow shocks, whose intermediate Mach number M_I=1, is obtained. In the hybrid simulation, the switch-off shock possesses a large-amplitude, left-hand-polarized rotational wave train of magnetic field in the downstream region. Each slow shock propagates to either lobe in the magnetotail. A strong temperature anisotropy with $T_{\parallel}>T_{\perp}$ appears in most region of the reconnection layer. This is due to the interpenetrating of ions between the two lobes and the backstreaming of ions from the downstream of each slow shock to the lobe. Second, the presence of a finite guide field in lobes ($B_y\neq 0$) is considered in the simulation. It is found that the slow shocks becomes nonswitch-off shocks with an intermediate Mach number $M_I<1$, and two rotational discontinuities are also present in the hybrid simulation to bound the reconnection layer from, respectively, the two lobes. In addition, our hybrid simulations show that the presence of the finite B_y destroys the coherent wave train in the reconnection layer if the lobe $B_{y0}\geq 0.08B_{x0}$. Finally, the simulations are extended to the asymmetric cases in which the plasma densities and/or the magnetic fields in the two lobes are unequal. For asymmetric cases with B_y=0 in the two lobes, it is found that an intermediate shock and a nonswitch-off slow shock are present in the reconnection layer and that the large-amplitude rotational wave structure does not exist in the entire reconnection layer if the density ratio between the two lobes $N_1/N_0\geq 1.5$, where N_0 and N_1 are the ion number densities in the two lobes, receptively. For general cases with both density asymmetry and $B_{y0}\neq 0$, two rotational discontinuities and two slow shocks are present in the reconnection layer, and the critical value of the density ratio, above which the coherent wave train does not exist, is reduced. The absence of a downstream wave train for the slow shocks observed in the magnetotail may be associated with the presence of a finite B_{y0}.

1. Introduction

In the Earth's magnetosphere, magnetic reconnection can take place at the magnetopause and in the magnetotail plasma sheet [*Dungey*, 1961]. This process plays an important role in the transfer of the solar wind mass, momentum, and energy into the Earth's magnetosphere at the magnetopause [e.g., *Russell and Elphic*, 1978] and the development of geomagnetic substorms and energy release in the magnetotail [*Hones*, 1979; *Schindler*, 1975].

Through magnetic reconnection, magnetic energy can be efficiently converted into plasma kinetic energy, leading to the ejection of a high-speed plasma. A layered structure which contains several magnetohydrodynamic (MHD) discontinuities and waves can be formed in the high-speed outflow region of magnetic reconnection [e.g., *Petschek*, 1964; *Levy et al.*, 1964; *Sonnerup et al.*, 1981; *Feldman et al.*, 1984; *Gosling et al.*, 1986; *Heyn et al.*, 1988; *Biernat et al.*, 1989; *Lin and Lee*, 1994a]. This layer is referred to as the reconnection layer. The energy conversion in the reconnection is mainly through the discontinuities and waves in the reconnection layer.

The formation and structure of the reconnection layer has been studied by resistive MHD simulations [*Shi and Lee*, 1990; *Lin et al.*, 1992; *Lin and Lee*, 1994a]. In general, intermediate shocks, time-dependent intermediate shocks (TDISs) [e.g., *Wu and Kennel*, 1992], slow shocks, slow expansion waves, and a contact discontinuity may exist in the reconnection layer at the magnetopause, where a large asymmetry in the magnetic field and plasma density is present across the current layer from the magnetosheath to the magnetosphere. On the other hand, in the symmetric magnetotail plasma sheet with equal magnetic field strength, equal plasma density, and antiparallel magnetic field (B_x) in the two lobes, two switch-off slow

Paper number 95JA01549.
0148-0227/95/95JA-01549$05.00

shocks are formed as a result of the magnetic reconnection at the distant tail X line, as in the *Petschek*'s [1964] reconnection model. Each of the two slow shocks propagates in either lobe/plasma sheet boundary layer. Across each slow shock, the tangential magnetic field decreases to zero from the lobe to the central plasma sheet, the plasma density is enhanced, and the plasma flow is greatly accelerated. The slow shock with a downstream tangential magnetic field equal to zero is called the switch-off shock. The intermediate Mach number, $M_I=V_{nu}/C_{Iu}$, is equal to 1 in the switch-off shock, where V_{nu} and C_{Iu} are, respectively, the normal flow speed and normal component of the Alfven velocity in the upstream region. Other slow shocks with $M_I<1$ are nonswitch-off shocks, whose downstream tangential magnetic field is nonzero. MHD simulations of the Petschek reconnection model has also been carried out by *Sato* [1979], *Ugai* [1984], and *Yan et al.* [1992].

To study the reconnection layer in collisionless plasmas in the magnetosphere, it is necessary to use a kinetic model. Recently, *Lin and Lee* [1993, 1994a, b] carried out one-dimensional (1-D) hybrid simulations of the reconnection layers at the dayside magnetopause and at the flank of the magnetopause. It is found that the result from the resistive MHD is modified. In the hybrid simulation, the TDIS quickly evolves to a steady rotational discontinuity, and the contact discontinuity cannot be identified because of the mixing of ions from the magnetosheath and the magnetosphere. Slow shocks and slow expansion waves are also modified. The simulation results are consistent with satellite observations at the magnetopause [e.g., *Sonnerup et al.*, 1981; *Gosling et al.*, 1986]. Note that the rotational discontinuities, instead of intermediate shocks or TDIS, are also present in the results from the ideal MHD formulation [*Kantrowitz and Petschek*, 1966; *Heyn et al.*, 1988; *Lin and Lee*, 1994a].

On the other hand, ISEE 3 deep-tail (~ $100R_E$) observations of the plasma and field data in the lobe/plasma sheet boundary layer often show a slow shock-like structure, with a decreased magnetic field, increased plasma density and temperature, and a large accelerated flow in the central plasma sheet [*Feldman et al.*, 1984, 1985; *Smith et al.*, 1984; *Schwartz et al.*, 1987]. According to the two-fluid theory, which includes ion inertial effects in the MHD theory, the slow shock should present a left-hand circularly polarized wave train of magnetic field, the ion cyclotron wave, in the downstream region [e.g., *Coroniti*, 1971]. This large-amplitude trailing wave train, however, has not been observed by the ISEE satellite. *Coroniti et al.* [1988] have further found that the observed wave amplitude of ion acoustic or lower-hybrid waves in the magnetotail is too small to damp the wave train. The lack of the large-amplitude wave train in the magnetotail slow shock has become a topic of recent research interest.

Swift [1983] and *Winske et al.* [1985] have carried out 1-D hybrid simulations for the switch-off shock ($M_I=1$). The results show the existence of the large-amplitude rotational wave train. *Lee et al.* [1989] have performed 1-D hybrid simulations for both switch-off ($M_I=1$) and nonswitch-off slow shocks ($M_I<1$). The initial profile in their model includes a finite shock transition region linking uniform upstream and downstream regions determined by the Rankine-Hugoniot (RH) jump conditions of the slow shock. It is found that there exists a critical number M_c such that for slow shocks with an intermediate Mach number $1\geq M_I>M_c$, a long, large-amplitude helical wave train appears in the downstream region, while for slow shocks with $M_I<M_c$, the downstream rotational wave is damped within a fraction of one wavelength. The critical Mach number is found to be M_c~0.98. It is suggested by *Lin and Lee* [1991, 1994a] that the damping of the downstream wave train and the ion heating of the slow shock are due to the chaotic ion orbits in the slow shock. On the other hand, *Omidi and Winske* [1989] have simulated the structure of slow shocks by letting the slow shock be formed from an incident plasma stream and a beam reflected off the boundary wall. It is found that the electromagnetic ion/ion cyclotron instability may play an important role in the damping of the downstream coherent wave train and ion heating of the slow shock [*Winske and Omidi*, 1990]. Hybrid simulations by *Vu et al.* [1992] show that switch-off slow shocks with or without a trailing wave train can be obtained by changing the downstream boundary conditions.

The above hybrid simulations were performed for an isolated slow shock, and the formation and structure of slow shocks in magnetic reconnection were not simulated. A recent hybrid simulation of the *Petschek* [1964] reconnection layer by *Fujimoto and Nakamura* [1994] shows that heavy ions may also play an important role in the damping of the wave train in the magnetotail slow shocks. The magnetotail reconnection layer, however, is not systematically studied. The guide field (B_y) is assumed to be exactly zero in the simulation, and the two lobes are assumed to be perfectly symmetric.

Satellite observations from magnetotail neutral sheet crossings often indicate that the dawn-dusk field component B_y is nonzero and maintains the same sign throughout all crossings [e.g., *Lui*, 1984]. It is suggested that the dawn-dusk component of the interplanetary magnetic field (IMF) penetrates partially (~13-50%) into the magnetotail [*King*, 1977; *Fairfield*, 1979]. In particular, the lobe B_y is also found to be frequently nonzero in the distant tail plasma sheet [*Tsurutani et al.*, 1984, 1987], and the contribution of the finite B_y to the structure of the lobe/plasma sheet boundary may be important.

In this paper, we extend our previous 1-D hybrid simulations of the Riemann problem associated with the magnetopause reconnection layer [e.g., *Lin and Lee*, 1993, 1994a] to the magnetotail and provide the structure of the lobe/plasma sheet boundary associated with magnetic reconnection in the distant tail. The hybrid simulations have been performed with the help of resistive MHD simulations.

Our previous MHD simulations [*Lin et al.*, 1992; *Lin and Lee*, 1994a] show that (1) the *Petschek* [1964] reconnection layer which contains two switch-off slow shocks ($M_I=1$) is formed in the case with symmetric lobes and with $B_y=0$, (2) the presence of a finite B_y reduces the intermediate Mach number (M_I) of the slow shocks in the symmetric reconnection layer and leads to the appearance of two additional TDISs (or rotational discontinuities in hybrid simulations), and (3) a slight asymmetry in plasma density or magnetic field on the two sides of the current layer lead to the disappearance of one slow shock and the changing of the intermediate Mach number in the other slow shock. Since both a nonzero guide field B_y and an asymmetry in field and plasma may be present in the tail lobes, we study (1) the effect of B_y and (2) the effect of slightly asymmetric lobe plasma and field on the distant tail reconnection layer. Whether a coherent wave train is present in the reconnection layer is also examined.

The outline of the paper follows. The simulation model is given in section 2. In section 3, we present our hybrid

simulation results, with the help of resistive MHD simulations. A summary is given in section 4.

2. Simulation Model

We study the structure of the reconnection layer which is formed because of the magnetic reconnection at the distant-tail X line between the two lobes. Initially, a current sheet separates the two lobes with antiparallel magnetic field components B_x in the x direction and a common guide magnetic field B_y in the y direction. The normal of the current sheet is along the z direction, and the current sheet is located at $z=z_c=0$. The total (thermal plus magnetic) pressure is balanced and the initial current sheet is a tangential discontinuity. At time $t=0$, a nonzero normal component of magnetic field $B_n=B_z$ is imposed in the system, corresponding to the occurrence of a magnetic reconnection in which B_n is present along the reconnected field lines. The initial current sheet then evolves to form the reconnection layer. A 1-D hybrid code is used to simulate the evolution of the initial current sheet and thus the structure of the reconnection layer. The 1-D initial value problem associated with the evolution of the current sheet is a Riemann problem [e.g., *Jeffrey and Taniuti*, 1964].

In the 1-D simulation, all the dependent variables are functions of the coordinate z and time t only. The MHD discontinuities and waves in the resulting reconnection layer propagates away from the initial current sheet to the lobes along the z direction. Note that our 1-D simulation results can be used to determine the two-dimensional (2-D) steady state reconnection layer in the xz plane [e.g., *Lin and Lee*, 1994a]. The quasi-steady reconnection may occur at the deep-tail X line during a quiet time. The time t in the 1-D model can be related to the x coordinate in the 2-D reconnection configuration by $x=\bar{v}_x t$, where $\bar{v}_x$ is approximately the accelerated plasma flow speed at the center ($z\sim0$) of the resulting reconnection layer. In the 2-D reconnection layer, all the discontinuities emanate from the point where the magnetic reconnection takes place.

The 1-D hybrid code used in this study is the one described by *Swift and Lee* [1983] and utilized by *Lee et al.* [1989] and *Lin and Lee* [1993, 1994a, b] in the simulations of the magnetopause reconnection layer and magnetotail slow shocks. In the hybrid model, ions are treated as particles and electrons as a massless fluid. The charge neutrality is assumed. In general, the magnetic field strength may not be equal in the two lobes, and neither the plasma density. In the simulation, the ion number density per grid, N, in the low-density lobe is chosen to be $N_0=25$, and the number density in the high-density lobe is $N_1=25$-50. In the following, the subscripts "0" and "1" represent the physical quantities in the lobes with, respectively, a relatively high plasma density and a low density.

The length per grid is chosen to be $0.158\lambda_0$, where $\lambda_0=c/\omega_{p0}$ is the ion inertial length in the low-density lobe, c is the speed of light, and ω_{p0} is the ion plasma frequency in the lobe. The simulation domain length is 4000 grids, with two buffer zones at, respectively, the two ends of the domain. The simulation results shown in this paper are only for the central part of the whole simulation domain, where the main reconnection layer exists.

A constant temperature is assumed across the initial current sheet. Thus for a given density asymmetry in the two lobes, the thermal pressure is also unequal in the lobes. The ratio of the magnetic field strengths in the two lobes is obtained from the condition of total pressure balance. In addition, the normal magnetic field component B_n, which is a constant in the 1-D model, is chosen to be $0.25B_{x0}$.

The initial profile of the x component magnetic field is given by

$$B_x(z) = 0.5(B_{x0}+B_{x1}) + 0.5(B_{x0}-B_{x1})\tanh[(z-z_c)/\delta] \quad (1)$$

where δ is the half width of the initial current sheet, which is chosen to be $2\lambda_0$. The guide field B_y is assumed to be constant across the initial current sheet. The profile of the thermal pressure P is determined by the total pressure balance

$$P(z) + B(z)^2/2\mu_0 = P_0(z) + B_0(z)^2/2\mu_0 \quad (2)$$

The initial profile of the ion number density is then determined from the pressure profile and the assumption of constant temperature. The flow velocity is assumed to be zero outside the initial current sheet.

The simulations have also been run for various initial profiles of physical quantities in the current sheet. The results of the Riemann problem are not quantitatively different from those shown in this paper.

In the hybrid simulation, the time is expressed in units of Ω_0^{-1}, where Ω_0 is the ion cyclotron frequency in the low-density lobe. The magnetic field is normalized to B_0, the ion number density to N_0, the pressure to the thermal pressure P_0 in the lobe, the velocity to the lobe Alfven speed V_{A0}, and the spatial coordinate is normalized to the ion inertial length λ_0.

To help us understand the hybrid simulation results, a 1-D resistive MHD is also used to simulate the magnetotail reconnection layer. An explicit two-step Lax-Wendroff scheme with a constant resistivity is utilized in the simulation. A detailed description of the MHD code can be found in the work by *Lin et al.* [1992]. In the MHD model, the spatial coordinate is normalized to the half width δ of the initial current sheet, and the time is normalized to $t_A\equiv\delta/V_{A0}$.

3. Structure of the Reconnection Layer in the Distant Magnetotail

In the following, first, we show the simulation result of the case with symmetric lobes and with a zero guide field ($B_y=0$) in the lobes. Second, simulations of symmetric cases with a nonzero lobe guide field ($B_y\neq0$) are shown, and the effects of the finite B_y on the tail reconnection layer are discussed. Finally, the effects of asymmetric plasma density and field in the two lobes on the reconnection layer are studied.

Seven cases are shown. Table 1 summarizes the structure of the tail reconnection layer for these seven cases with various symmetry conditions and common guide field B_{y0} in the lobes. We have also simulated the cases with a finite inflow speed of 0.1-$0.2V_{A0}$ at the boundaries. The resulting structure of the reconnection layer is nearly the same as in the cases without the inflow.

3.1. Symmetric Lobes with $B_y=0$

In case 1, the magnetic field strengths in the two lobes are equal, and so are the plasma densities, with $N_1=N_0$ and $B_1=B_0$. The magnetic fields are exactly antiparallel on the two sides of the initial current sheet, with $B_{y1}=B_{y0}=0$ in the lobes. The lobe plasma beta is assumed to be $\beta_1=\beta_0=0.1$, and the electron to ion temperature ratio $T_e/T_i=0$.

Table 1. Summary of Hybrid Simulation Results

	Symmetry Condition	B_{y0}	Structure of the Reconnection Layer
Case 1	symmetric	0	switch-off SS + switch-off SS; wave train
Case 2	symmetric	$0.1B_{x0}$	RD + SS + SS + RD; no wave train
Case 3	symmetric	$0.2B_{x0}$	RD + SS + SS + RD; no wave train
Case 4	symmetric	$0.5B_{x0}$	RD + RD; no wave train
Case 5	asymmetric: $N_1=1.2N_0$	0	IS (with wave train) + SS (with wave train)
Case 6	asymmetric: $N_1=1.4N_0$	0	IS (with wave train) + SS (no wave train)
Case 7	asymmetric: $N_1=2N_0$	0	IS (no wave train) + SS (no wave train)
Other	asymmetric	$\neq 0$	RD + SS + SS' + RD'

Note: SS, slow shock; RD, rotational discontinuity; IS, intermediate shock. The wave train is that associated with a large-amplitude, circularly-polarized wave in magnetic field. For cases with symmetric lobes, the coherent wave train does not exist if $B_{y0}/B_{x0}\geq 0.8$. For asymmetric cases with $B_{y0}=0$, the coherent wave does not exist if $N_1/N_0\geq 1.5$. For general cases with both a finite lobe B_{y0} and an asymmetric plasma density, the critical number of density ratio N_1/N_0 decreases.

Figure 1a shows the simulation results of case 1 by using the 1-D resistive MHD [e.g., *Lin et al.*, 1992]. Two slow shocks (SSs) are present in the reconnection layer, whose positions are plotted in the right column of Figure 1a as a function of time t. These two slow shocks propagate toward the two lobes, respectively. The middle column of Figure 1a shows spatial profiles of B_x, B_y, plasma density ρ, magnitude of the tangential magnetic field B_t, temperature T, thermal pressure P, and plasma flow velocities (V_x, V_y, and V_z). The values shown are for the normalized quantities. The time corresponding to these spatial profiles is indicated by the arrow on the vertical axis of the right plot. The hodogram of tangential magnetic field is shown in the left column. Across each slow shock from upstream to downstream, the magnetic field strength is reduced to zero, as shown in the spatial profile plots. The shock is a switch-off shock with an intermediate Mach number $M_I=1$. The plasma density, temperature, and flow speed increase across the slow shock.

In addition, two fast expansion (FE) waves are also present in the simulation, as shown by the two dashed lines in the right column of Figure 1a. These fast waves, however, quickly propagate away from the main reconnection layer.

The hybrid simulation of case 1 is shown in Figure 2. The left column of Figure 2 presents, from the top, spatial profiles of B_x, B_y, magnetic field magnitude B, and ion number density N at time $t=600\Omega_0^{-1}$. The right column shows the profiles of ion temperatures parallel ($T_\parallel$) and perpendicular ($T_\perp$) to the magnetic field, the x component velocities of ion particles in the v_{ix}-z phase space, and the y component velocities of ions in the v_{iy}-z phase space, where v_{ix} and v_{iy} represent, respectively, the x velocity and y velocity of ion particles. The hodogram of tangential magnetic field at $t=600\Omega_0^{-1}$ in case 1 is shown in Figure 3a.

Same as in the MHD simulation, two switch-off slow shocks with $M_I=1$ are formed in the reconnection layer, where the intermediate Mach number $M_I=V_{nu}/C_{Iu}$, the intermediate mode speed in upstream $C_{Iu}=[B_u/(\mu_0\rho_u)^{1/2}][1-(\beta_\parallel-\beta_\perp)/2]^{1/2}$, ρ_u is the upstream plasma density, and $\beta_\parallel$ and $\beta_\perp$ are, respectively, the upstream plasma beta parallel and perpendicular to the magnetic field. The shock fronts of the two slow shocks are indicated in Figure 2 by a and b, respectively, with shock a propagating in the $-z$ direction and shock b in the $+z$ direction. The ion number density, perpendicular temperature, and flow speed increase across the slow shock, while the strength of magnetic field decreases. In the hybrid simulation, these slow shocks exhibit a large-amplitude, left-hand-polarized helical wave train in magnetic field in the downstream region, as seen from B_x and B_y profiles in Figure 2 and the magnetic field hodogram in Figure 3a. The fluctuation of the downstream magnetic field is around $B_t=0$, where B_t is the tangential magnetic field. The presence of the large-amplitude rotational wave train in switch-off shocks has also been found in the hybrid simulations by *Swift* [1983], *Winske et al.* [1985], *Lee et al.* [1989], *Lin and Lee* [1994a], and *Fujimoto and Nakamura* [1994], consistent with the two-fluid theory of slow shocks [e.g., *Coroniti*, 1971].

The plasma temperature parallel to the magnetic field ($T_\parallel$) is found to increase in most regions, except the center (z~0), of the reconnection layer. This is due to the interpenetrating of ions between the two lobes and the backstreaming of ions from downstream to upstream of the slow shock. It is seen from the phase-space plots of ion velocities in Figure 2 that there exists a beam of ions propagating upstream of each slow shock. The beam in each lobe contains approximately half of the backstreaming ions from the downstream of the slow shock and half of the transmitted ions from the other lobe. The presence of the ion beams upstream of the slow shocks in the magnetotail reconnection layer has also been reported by *Fujimoto and Nakamura* [1994], and the backstreaming of ions from the slow shock to upstream and the increase of the parallel temperature have also been found by *Swift* [1983], *Winske et al.* [1985], *Lee et al.* [1989], and *Omidi and Winske* [1989]. The increase of plasma density across the slow shocks in Figure 2 is not as large as in the MHD simulation because of the temperature anisotropy with $T_\parallel > T_\perp$. The firehose marginal stability condition, $\beta_\parallel-\beta_\perp=2$, is nearly satisfied in the transition region of the slow shock. Upstream of the shock, $\beta_\parallel-\beta_\perp$~1.1, while in the far downstream at the center of the reconnection layer, $\beta_\parallel-\beta_\perp$~ −1.

In the upstream region of each slow shock, the tangential magnetic field has a small fraction of right-hand polarization, which attaches the large downstream wave rotations, as shown in the hodogram of the tangential field. This weak Alfven mode pulse develops in the simulation to conserve the total B_y in the whole simulation domain.

3.2. Symmetric Lobes With $B_y\neq 0$

Next, we study the cases with $B_y\neq 0$ in the two lobes. Figures 1b and 1c show MHD simulations of cases 2 and 4,

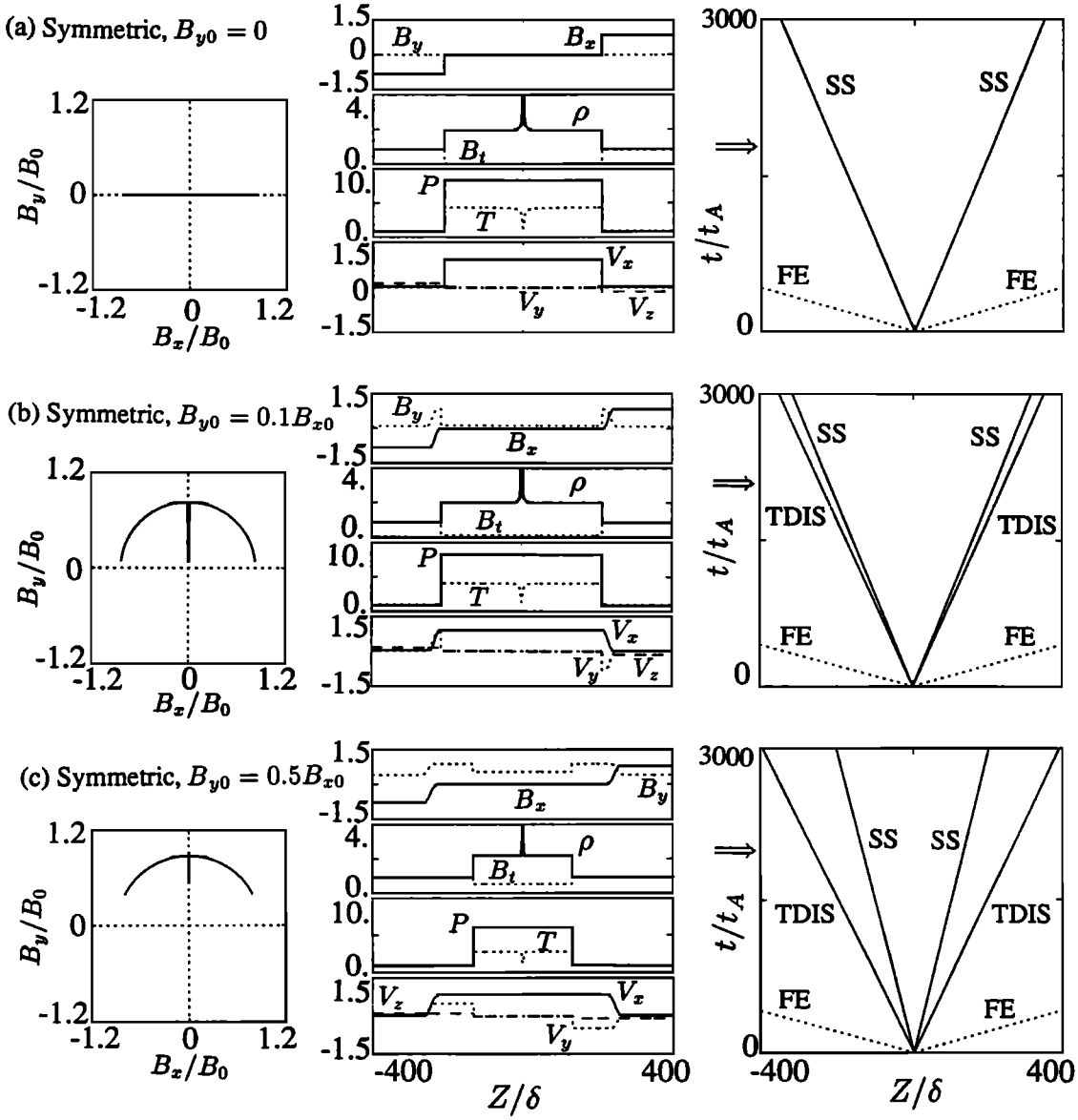

Figure 1. MHD simulation results of symmetric cases: (a) case 1 with B_{y0}=0, (b) case 2 with B_{y0}=0.1B_{x0}, and (c) case 4 with B_{y0}=0.5B_{x0}. The right column shows positions of the MHD discontinuities as a function of the time t. The middle column presents spatial profiles of B_x, B_y, plasma density ρ, tangential magnetic field B_t, temperature T, thermal pressure P, and plasma flow velocities V_x, V_y, and V_z. The values shown are for the normalized quantities. The time corresponding to the spatial profiles in each case is indicated by the arrow on the t axis of the right plot. The left column shows the hodograms of tangential magnetic field. The slow shock, time-dependent intermediate shock, and fast expansion wave are indicated by SS, TDIS, and FE, respectively.

respectively. In case 2, the lobe guide field B_{y1}=B_{y0}=0.1B_{x0}, while in case 4 B_{y1}=B_{y0}=0.5B_{x0}. In these two cases, the lobe plasma beta is the same as in case 1, with β_1=β_0=0.1. Since the MHD result of case 3, with symmetric lobes and B_{y1}=B_{y0}=0.2B_{x0}, is very similar to that of case 2, we do not show the MHD simulation of case 3.

As shown in the right column of Figure 1b, four discontinuities can be identified in the main reconnection layer of case 2. Two time-dependent intermediate shocks (TDISs) bound the reconnection layer from the two lobes, respectively. Behind each TDIS, there propagates a slow shock (SS) toward each lobe side in the reconnection layer. At each TDIS, the upstream and downstream magnetic fields are noncoplanar with the normal vector. The tangential magnetic field rotates by 84° across the TDIS, from the lobe value to the downstream value with B_z=0, as seen from the field hodogram in the left column. This is a 2-3 TDIS, whose upstream normal flow speed is subfast and superintermediate and downstream normal flow speed is subintermediate and superslow. The thickness of the TDIS increases with time as $t^{1/2}$, and the strength decreases [e.g., *Lin et al.*, 1992]. As $t\rightarrow\infty$, the TDIS evolves to a rotational discontinuity with an infinite width. Note that in the ideal MHD without dissipation, the TDIS is replaced by a steady rotational discontinuity [e.g., *Lin and Lee*, 1994a].

At the time shown in Figure 1b, the TDIS and SS on each side has been separated. At each of the two slow shocks, the coplanarity condition of magnetic field is satisfied with B_z=0.

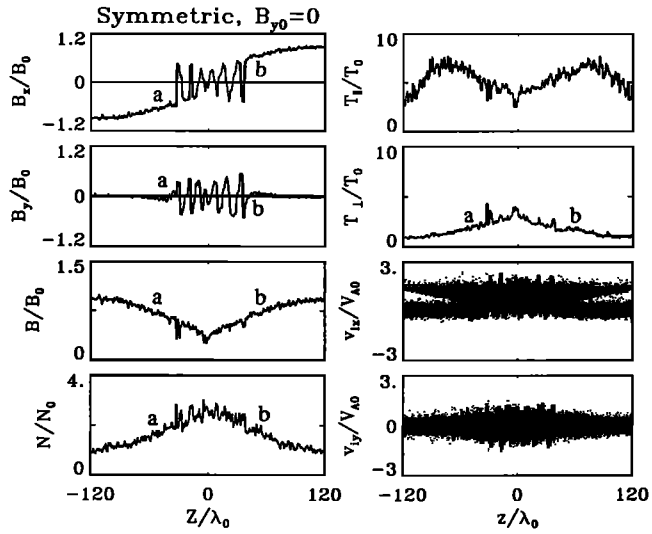

Figure 2. Hybrid simulation results of case 1 at time t=600Ω_0^{-1}. The left column presents, from the top, spatial profiles of B_x, B_y, magnetic field magnitude B, and ion number density N. The right column shows the profiles of ion temperatures parallel ($T_\parallel$) and perpendicular ($T_\perp$) to the magnetic field, the x component velocities of ion particles in the v_{ix}-z phase space, and the y component velocities of ions in the v_{iy}-z phase space. The shock fronts of two slow shocks are indicated by a and b, respectively.

Across the slow shock, the plasma density increases and magnetic field decreases. Different from the slow shocks in case 1, the downstream tangential magnetic field is nonzero, as shown in Figure 1b, and the slow shock is a nonswitch-off shock. A close examination indicates that the intermediate Mach M_I=0.95 at the slow shock in case 2. Note that in early times of the simulation run when the TDIS and SS has not been separated, the tangential magnetic field has a smaller fraction of rotation across the two discontinuities than that shown in the hodogram of Figure 1b. This result will be further demonstrated below in the presentation of the hybrid simulations.

The MHD result of case 4 is similar to that of case 2, as shown in Figure 1c. Two TDISs and two SSs are present in the reconnection layer. At the TDIS, the rotation angle of tangential magnetic field is 63°. Our study shows that as the guide field B_{y0} increases, the intermediate Mach number M_I of the slow shocks decreases. As seen in Figure 1c, the strength of the slow shocks in case 4 is weaker than that in case 2, and the downstream tangential magnetic field is larger. The intermediate Mach number of the slow shocks in case 4 is found to be M_I=0.72.

We now present the hybrid simulation results for symmetric cases with a finite lobe B_y. Figure 4 shows spatial profiles of N, B_y, B_x obtained from the hybrid simulation of case 2 with B_{y1}=B_{y0}=0.1B_{x0}. The profiles shown are for a time series from t=0 to t=640Ω_0^{-1}. Hodograms of tangential magnetic field at t=120, 200, 320, and 600Ω_0^{-1} are also plotted in Figure 4.

Four discontinuities are present in the main reconnection layer of case 2. A rotational discontinuity propagates along trajectory pp' to one lobe, followed by a slow shock along qq', as shown in the B_y and B_x profiles in Figure 4. To the other lobe, there propagates another rotational discontinuity along uu', behind which is a slow shock along rr'. In the hybrid simulation, the two rotational discontinuities play the role of time-dependent intermediate shocks in the MHD result. The existence of rotational discontinuities in hybrid simulations has also been found in our previous studies of the magnetopause reconnection layer [*Lin and Lee*, 1993, 1994a, b].

At early times of the simulation run, the rotational discontinuity and slow shock on either side of the reconnection layer are not separated. As shown in the magnetic field hodograms at t=120 and 200Ω_0^{-1}, the rotation of tangential magnetic field across either side appears flatter than at later times (e.g., t= 600Ω_0^{-1}) when the discontinuities are separated. As mentioned in section 2, the time t in the 1-D simulation may correspond to the spatial distance x from the point where the reconnection takes place in the 2-D steady reconnection configuration. At a distance x close to the reconnection point in the 2-D configuration, the z profiles of physical quantities are similar to the profiles in the 1-D simulation at an early time. The z profiles at a farther x distance are similar to the 1-D profiles at a later time. Likewise, the hodograms of early (later) times shown in Figure 4 correspond to those at close (larger) x distances from the reconnection point.

At t>360Ω_0^{-1}, the rotational discontinuity and slow shock on each side of the reconnection layer are separated. As shown in the B_y and B_x profiles and field hodograms at t=600Ω_0^{-1}, across the rotational discontinuity on the z<0 (z>0) side, the magnetic field rotates from the lobe value indicated by a (f) to B_x~0 at b (e), similar to the MHD result in Figure 1b. Because of the presence of the temperature anisotropy in the reconnection layer, the plasma density increases and the magnetic field decreases across the rotational discontinuity [see *Lin and Lee*, 1994a]. It is found that the RH jump

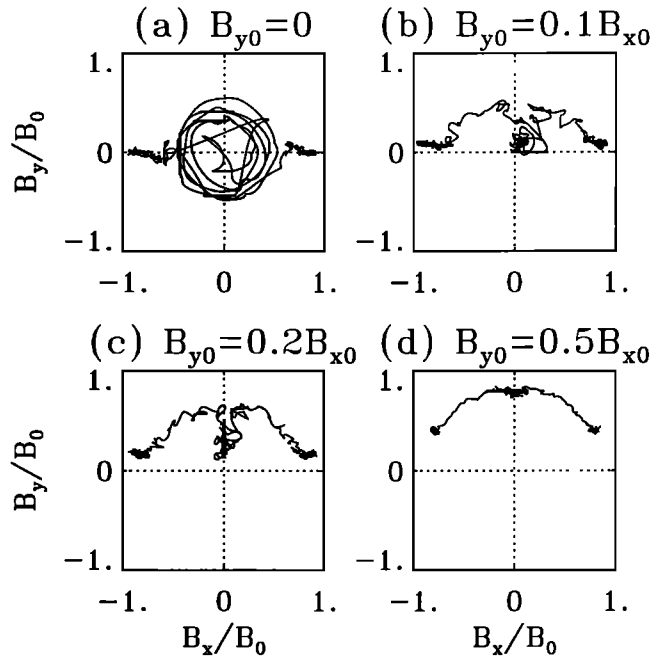

Figure 3. Hodograms of tangential magnetic field for cases 1-4, with the lobe guide field B_{y0}=0, 0.1, 0.2, and 0.5B_{x0}, respectively. Large-amplitude rotational waves are present in the case with B_{y0}=0, while it does not exist in the other three cases with a finite B_{y0}.

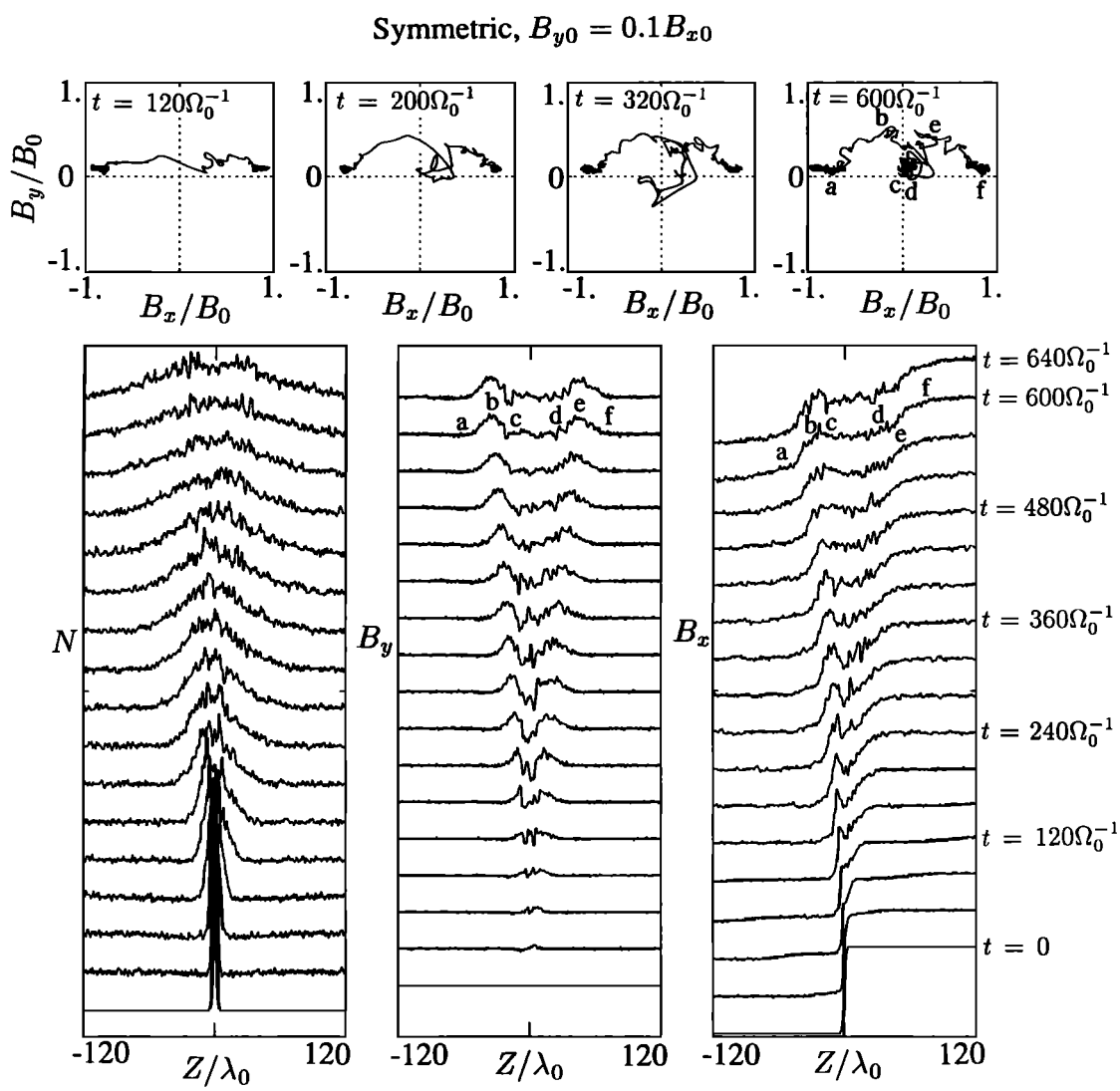

Figure 4. Spatial profiles of N, B_y, B_z obtained from the hybrid simulation of case 2 with B_{y0}=0.1B_{x0}. The profiles shown are for a time series from t=0 to t=640Ω_0^{-1}. Hodograms of tangential magnetic field at t=120, 200, 320, and 600Ω_0^{-1} are also plotted.

conditions of rotational discontinuity [e.g., *Hudson*, 1971] are satisfied at the rotational discontinuities in case 2.

Across the slow shock on the z<0 (z>0) side in Figure 4, the magnetic field decreases from a large B_y as indicated by *b* (*e*), which is in the downstream region of the rotational discontinuity, to B_y~0.1B_{x0} at *c* (*d*). The component B_z remains ~0 across the slow shock, as in the MHD simulation of case 2. Different from the MHD result, the ion density only slightly increases across the slow shock, which is due to the modification of RH jump conditions at the slow shock by the temperature anisotropy [e.g., *Lin and Lee*, 1994a]. The intermediate Mach number of the nonswitch-off slow shock is found to be M_I~0.95.

One feature that is not observed in the slow shocks in case 2 is the large-amplitude rotational wave train, which appears in the switch-off shock in case 1. Figure 3 shows hodograms of magnetic field for cases 1-4, with the lobe guide field B_{y0}=0, 0.1, 0.2, and 0.5B_{x0}, respectively. It is seen that the large-amplitude rotational waves exist in case 1 with B_{y0}=0, in which two switch-off slow shocks are present, as described earlier. In cases 2 and 3, two rotational discontinuities are present in addition to two slow shocks, and the slow shocks are nonswitch-off shocks as seen in Figure 3. There exists no wave train in these two cases with a finite lobe B_y. In case 4 with a larger B_{y0}, the slow shocks in the hybrid simulation are too weak to be identified. Notice that these slow shocks are much weaker than in the MHD simulation, which is due to the presence of the temperature anisotropy in the hybrid simulation.

We have also simulated the cases with B_{y0}=0.05, 0.07, 0.08, and 0.09B_{x0}. The result of the case with B_{y0}=0.05B_{x0} is very similar to case 1. The slow shock is near switch-off, with a large-amplitude helical wave train. While B_{y0} increases to 0.08B_{x0} or larger, the intermediate Mach number M_I is smaller than a critical number M_C~0.98, and the coherent wave train disappears in the nonswitch-off slow shocks. The present result is consistent with our earlier study which shows that the downstream wave train is absent in nonswitch-off slow shocks with M_I<M_C~0.98 [*Lee et al.*, 1989; *Lin and Lee*, 1991].

The results shown above indicate that a finite lobe guide field B_{y0} (≥0.08B_{x0}) reduces the intermediate Mach number of the formed slow shocks below the critical Mach number

($M_I<M_C$~0.98), which leads to the disappearance of the large-amplitude helical wave train.

3.3. Reconnection Layer in the Magnetotail With Asymmetric Lobes

Finally, we study the cases with different plasma densities and different magnetic fields in the two lobes. The cases with $B_{yl}=B_{y0}=0$ are shown. For the asymmetric cases with $B_y\neq0$ in the lobes, the results are similar to the symmetric cases with $B_y\neq0$, with two rotational discontinuities and two nonswitch-off slow shocks present in the reconnection layer. The two rotational discontinuities (two slow shocks) are, however, not identical.

Figure 5 shows the MHD simulation results of case 5, in which $\rho_1=1.2\rho_0$, $B_1=0.99B_0$, and $\beta_0=0.1$. Three discontinuities can be identified in the main reconnection layer, as shown in the right plot of Figure 5. An intermediate shock (IS) propagates to the high-density lobe ($z<0$), a slow shock (SS) to the low-density lobe ($z>0$), and a contact discontinuity (CD) exists at the center of the reconnection layer. The spatial profiles of various quantities are shown in the left plot. The intermediate Mach number at IS is M_I~1.02, and that at SS is M_I~0.98. The tangential magnetic field at the center of the reconnection layer is nonzero, different from the symmetric case shown in Figure 1a. Across the intermediate shock, the tangential magnetic field changes from B_x~$-0.98B_0$ in upstream to B_x~$0.07B_0$ in downstream, with its sign reversed. The plasma density and flow speed increase across IS. Across the contact discontinuity CD, the plasma density changes, while pressure and magnetic field are conserved.

In addition, two fast expansion waves (FE and FE') are also present in the simulation, as shown in the right column of Figure 5.

The hybrid simulation results of case 5 are shown in Figure 6a. Plotted in Figure 6a are the hodogram of tangential magnetic field and the spatial profiles of B_x, B_y, and N at $t=640\Omega_0^{-1}$. The upstream state of the intermediate shock IS is indicated by a and downstream by b. A wave structure appears downstream of the intermediate shock, with nearly two left-hand rotations of magnetic field around B_x~$0.05B_0$ and $B_y=0$. The number of the rotation does not increase in later times of the simulation run. On the other hand, there also appears a left-hand rotation of magnetic field in the near switch-off slow shock SS, whose upstream is indicated by d and downstream by c as shown in Figure 6a. No contact discontinuity can be identified because of the mixing of ions from both sides of the reconnection layer. A recent study by *Wu et al.* [1994] shows that the contact discontinuity can exist in hybrid simulations if $T_e/T_i\geq0.5$.

As the density asymmetry N_1/N_0 increases, the variation of magnetic field across the slow shock becomes smaller. Figure 6b shows the hybrid simulation results of case 6 at $t=760\Omega_0^{-1}$, with $N_1=1.4N_0$ and $B_1=0.98B_0$. Similar to case 5, an intermediate shock and a nonswitch-off slow shock are present in the reconnection layer. The upstream and downstream of the intermediate shock are labeled by a and b, respectively, and those of the slow shock are indicated by d and c respectively. It is seen that the magnetic field in the downstream region of the intermediate shock, which is also the downstream magnetic field of the slow shock, is B_x~$0.15B_0$. The slow shock does not possess a large-amplitude rotation of the magnetic field.

As the density ratio increases to be greater than a critical value, N_1/N_0~1.5, the rotational wave structure disappears in the entire reconnection layer. Figure 6c shows the results of case 7 at $t=720\Omega_0^{-1}$, in which $N_1=2N_0$ and $B_1=0.95B_0$. The magnetic field changes by 180° across the intermediate shock from a to b. Through the slow shock from d to c, B_x monotonically decreases, while B_y almost remains zero.

In the general cases with both $N_1\neq N_0$ and $B_{y0}\neq0$, the critical value of N_1/N_0, above which the coherent wave train disappears, is reduced.

4. Summary and Discussion

One-dimensional resistive MHD and hybrid simulations have been performed to study the structure of the reconnection layer in the magnetotail. First, the case with equal magnetic field strengths, equal plasma densities, and antiparallel magnetic fields in the two lobes are simulated. Second, the presence of a finite guide field B_y in lobes is considered, and

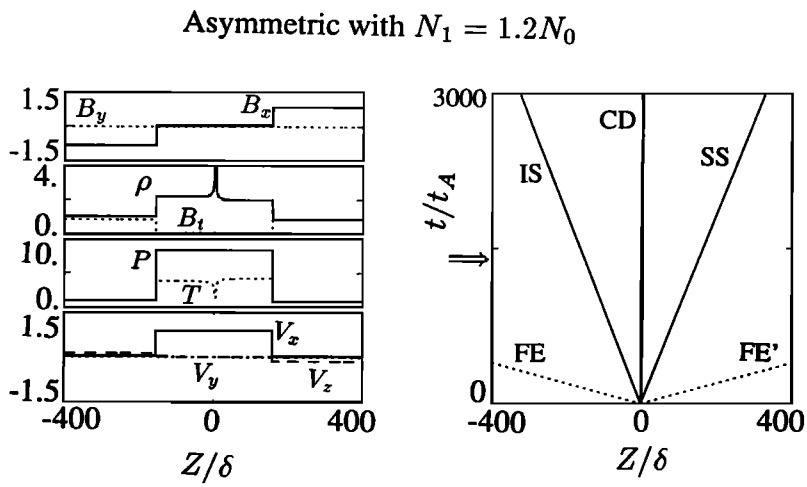

Figure 5. MHD simulation results of case 5 with $\rho_1=1.2\rho_0$ and $B_1=0.99B_0$. The spatial profiles of various quantities are shown in the left column, while positions of the intermediate shock (IS), contact discontinuity (CD), and slow shock (SS) as a function of time t are shown in the right plot.

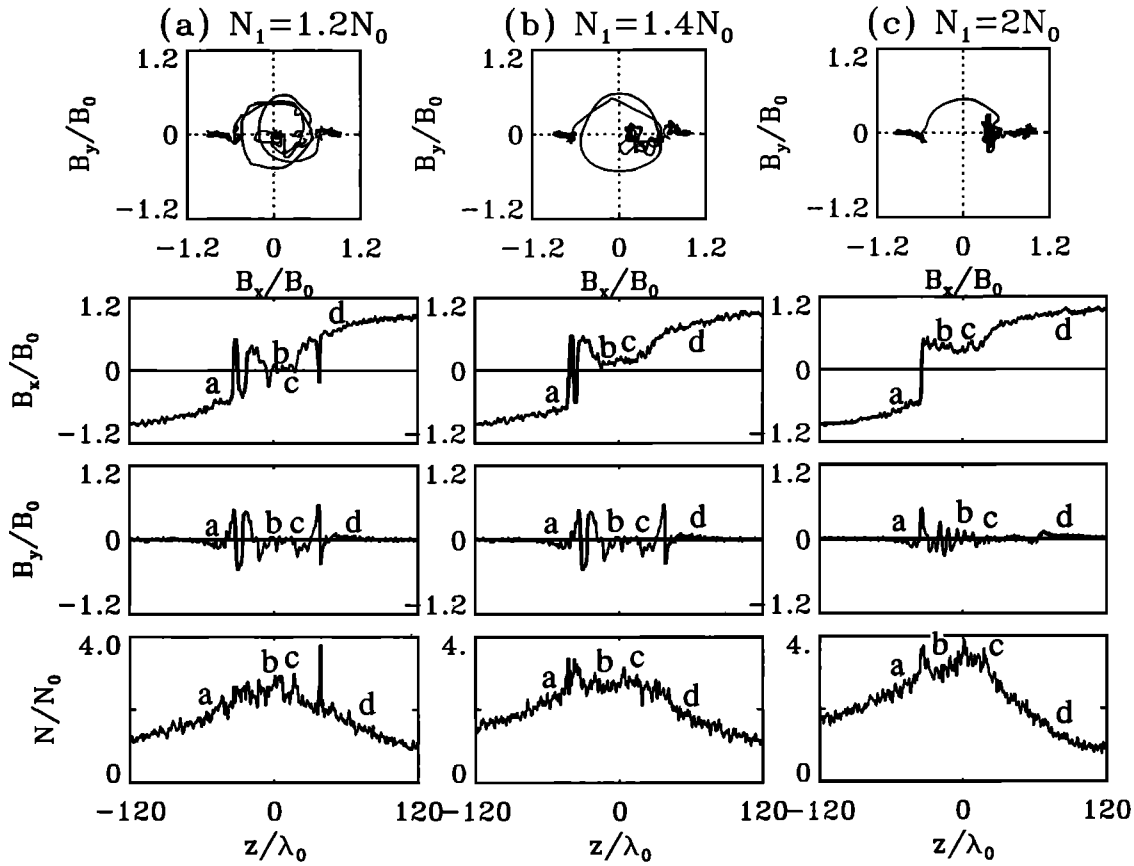

Figure 6. Hybrid simulation results of (a) case 5 with $N_1=1.2N_0$ and $B_1=0.99B_0$ at $t=640\Omega_0^{-1}$, (b) case 6 with $N_1=1.4N_0$ and $B_1=0.98B_0$ at $t=750\Omega_0^{-1}$, and (c) case 7 with $N_1=2N_0$ and $B_1=0.95B_0$ at $t=720\Omega_0^{-1}$. Plotted are hodograms of tangential magnetic field and spatial profiles of B_x, B_y, and N. The guide field $B_{y1}=B_{y0}=0$ in these cases.

the effects of the lobe B_y on the reconnection layer is investigated. Finally, the simulations are extended to the asymmetric cases in which the plasma densities and/or the magnetic fields in the two lobes are unequal. A brief summary of the simulation results is given below.

1. In the case with symmetric lobes and with $B_{y0}=0$ in the lobes, the *Petschek* [1964] reconnection layer which contains two switch-off slow shocks ($M_f=1$) is obtained. In the hybrid simulation, the switch-off shock possesses a large-amplitude, left-hand polarized rotational wave train in magnetic field in the downstream region. Each slow shock propagates to either lobe in the magnetotail. The results are consistent with earlier simulations of switch-off shocks by *Swift* [1983], *Winske et al.* [1985], *Lee et al.* [1989], *Lin and Lee* [1991], and *Fujimoto and Nakamura* [1994].

2. In the symmetric cases with a lobe $B_{y0}\neq 0$, the slow shocks becomes nonswitch-off shocks with $M_f<1$. In addition, two rotational discontinuities are also present in the hybrid simulation to bound the reconnection layer from, respectively, the two lobes. In the resistive MHD simulations, however, two time-dependent intermediate shocks, instead of the rotational discontinuities, are formed in the reconnection layer. Our hybrid simulations show that for $B_{y0}\geq 0.08B_{x0}$, the intermediate Mach number M_I of the slow shock becomes smaller than a critical Mach number $M_C\sim 0.98$ and the large-amplitude wave train disappears. Therefore the presence of a finite B_y in the lobes may destroy the coherent wave train in the symmetric reconnection layer.

3. A slight asymmetry in plasma density and/or magnetic field in the two lobes leads to the disappearance of one slow shock in the reconnection layer. In addition, the other slow shock, which exists on the low-density side, becomes a nonswitch-off shock. In the MHD simulation, a contact discontinuity exists at the center of the reconnection layer. In the hybrid simulation, however, the contact discontinuity cannot be identified because of the mixing of ions from two lobes. For the density ratio $N_1/N_0\geq 1.5$, our hybrid simulations show that the large-amplitude rotational wave structure disappears in the entire reconnection layer.

4. In the general cases with both density asymmetry and $B_{y0}\neq 0$, the critical value of N_1/N_0, above which the coherent wave train disappears, is reduced.

5. A strong temperature anisotropy with $T_\parallel > T_\perp$ appears in most region of the reconnection layer. This is due to the interpenetrating of ions between the two lobes and the backstreaming of ions from downstream to upstream through the MHD shocks. The strengths of the slow shocks, rotational discontinuities, and intermediate shocks in the hybrid simulations may be different from those in the MHD simulations because of the presence of the temperature anisotropy.

The hybrid simulation indicates that the structure of the magnetotail reconnection layer is sensitive to the guide magnetic field B_y in the lobes. The presence of the guide field can bring rotational discontinuities into the reconnection layer, change switch-off slow shocks in the *Petschek* [1964]

reconnection model to nonswitch-off shocks, and lead to the disappearance of the coherent wave trains in the reconnection layer.

At the dayside magnetopause, it is observed that a finite guide field is present in the plasmoids associated with the flux transfer events (FTEs) [e.g., *Russell and Elphic*, 1978], and that the core magnetic field is enhanced at the center of the magnetic flux tube [*Postman et al.*, 1982]. The guide field in the plasmoids is believed to be associated with a finite guide field in the IMF [e.g., *Lee and Fu*, 1985; *Scholar*, 1988]. In the magnetotail, the existence of B_y within the plasmoids has also been observed [e.g., *Sibeck et al.*, 1984; *Scholar et al.*, 1985; *Noshed et al.*, 1986; *Frank et al.*, 1994]. *Hughes and Sibeck* [1987] have compared observations of B_y within plasmoids and related tail structures with simultaneous upstream IMF B_y data. It is concluded that the B_y within plasmoids may also result from the penetration of the IMF B_y field. The presence of the finite B_y in the distant tail (~100-200R_E) lobe has also been reported [*Tsurutani et al.*, 1984, 1987; *Yamamoto et al.*, 1994].

It is suggested that the B_y component of the IMF penetrates ~13-50% into the magnetotail [*King*, 1977; *Fairfield*, 1979; *Lui*, 1984]. For a magnitude of IMF B_y~5 nT, this may correspond to B_{y0}~0.65-2.5 nT in the tail lobes. Taking an average field strength in the distant tail lobes to be B_0~10 nT, this guide field B_{y0}~0.07-25B_0. From the simulations shown in this paper, the coherent wave train does not exist if $B_{y0} \geq 0.08 B_{x0}$. Therefore our study suggests that the lack of the wave train in the magnetotail may be due to the existence of a finite B_y in the lobes.

Our hybrid simulations show that the lack of the coherent wave train in the reconnection layer is related to the intermediate Mach number (or the magnitude of downstream tangential magnetic field) of slow shocks. As the guide field B_{y0} increases, the intermediate Mach number decreases from M_I=1 in switch-off shocks while B_{y0}/B_{x0}=0 to M_I<1 while $B_{y0}/B_{x0} \neq 0$. The large-amplitude rotational wave train disappears as the intermediate Mach number decreases to be smaller than a critical number M_C~0.98. Likewise, in the asymmetric cases, the coherent wave disappears as the density ratio N_1/N_0 increases, which corresponds to the decrease of the intermediate Mach number M_I at the slow shock. It is noticed that *Lee et al.* [1989] also found from hybrid simulations that the large-amplitude coherent wave train does not exist in the magnetotail slow shock if M_I is smaller than a critical number M_C~0.98. Their simulations, though is for an isolated slow shock, seem to be consistent with the present simulation study for the tail reconnection layer.

Our 1-D simulation results can be used to determine the 2-D structure of the reconnection layer in the steady-state reconnection. The 1-D z profiles at various times t corresponds to the z profiles at various distances x, in the 2-D configuration, from the X line. At a distance x not far enough from the X line, the MHD discontinuities in the reconnection layer may not be clearly separated, and the profiles of physical quantities may look like a combination of various discontinuities. The quasi-steady reconnection may take place in the distant magnetotail during a quiet time.

In addition to the presence of B_{y0} and small density asymmetry in the two lobes, another possibility that may cause the lack of the coherent wave train in the magnetotail reconnection is related to the 2-D configuration of the reconnection which is not in a perfect steady state. A 2-D MHD simulation of the Petschek-type reconnection layer by *Lee et al.* [1989] suggests that because of the 2-D effects, the slow shocks formed the magnetotail are likely to be nonswitch-off shocks with M_C<0.98, while they are expected to be switch-off shocks in the steady state model.

It should be noticed that the concept of the critical Mach number used, as described in this paper, to delineate between solutions with and without downstream wave train is still controversial. Alternative explanations have also been offered by other authors [e.g., *Omidi and Winske*, 1989; *Winske and Omidi*, 1990; *Vu et al.*, 1992; *Fujimoto and Nakamura*, 1994], as mentioned in previous sections. In addition, the 2-D effects on the structure of reconnection layer remain to be solved, which will be investigated in our future study.

While the deep-tail reconnection layer may be associated with a quasi-steady reconnection, the near-Earth reconnection during a substorm active time may correspond to the transient stage of a 2-D reconnection configuration. The structure of the near-Earth reconnection layer is observed to be very different from the structure of the deep-tail reconnection layer [e.g., *Cattell et al.*, 1992; *Feldman et al.*, 1987]. The near-Earth reconnection layer is beyond the scope of this paper.

Acknowledgments. This work was supported by NSF grant ATM-9507993 to the Auburn University and DOE grant DE-FG06-91ER 13530 and NASA SPTP grant NAG5-1504 to the University of Alaska. Computer resources were provided by the Alabama Supercomputer Network and Pittsburgh Supercomputing Center.

The Editor thanks K. B. Quest for the assistance in evaluating this paper.

References

Biernat, H. K., M. F. Heyn, R. P. Rijnbeek, V. S. Semenov, and C. J. Farrugia, The structure of reconnection layers: Application to the Earth's magnetopause, *J. Geophys. Res.*, *84*, 287, 1989.

Cattell, C. A., C. W. Carlson, W. Baumjohann, and H. Luhr, The MHD structure of the plasma sheet boundary, 1, tangential momentum balance and consistency with slow mode shocks, *Geophys. Res. Lett.*, *19*, 2083, 1992.

Coroniti, F. V., Laminar wave-train structure of collisionless magnetic slow shocks, *Nuclear Fusion*, *11*, 261, 1971.

Coroniti, F. V., F. L. Scarf, C. F. Kennel, B. T. Tsurutani, and E. J. Smith, A search for lower hybrid drift turbulence in slow shocks, *J. Geophys. Res*, *93*, 2553, 1988.

Dungey, J. W., Interplanetary magnetic field and the auroral zones, *Phys. Rev. Lett.*, *6*, 47, 1961.

Fairfield, D. H., On the average configuration of the geomagnetic tail, *J. Geophys. Res.*, *84*, 1950, 1979.

Feldman, W. C., S. J. Schwartz, S. J. Bame, D. N. Baker, J. Birn, J. T. Gosling, E. W. Hones Jr., D. J. McComas, J. A. Slavin, E. J. Smith, and R. D. Zwickl, Evidence for slow-mode shock in the deep geomagnetic tail, *Geophys. Res. Lett.*, *11*, 599, 1984.

Feldman, W. C., D. N. Bakes, S. J. Bame, J. Birn, J. T. Gosling, E. W. Hones, Jr., and S. J. Schwartz, Slow-mode shocks: A semipermanent feature of the distant geomagnetic tail, *J. Geophys. Res.*, *90*, 233, 1985.

Feldman, W. C., R. L. Tokas, J. Birn, E. W. Hones, Jr., S. J. Bame, and C. T. Russell, Structure of a slow mode shock observed in the plasma sheet boundary layer, *J. Geophys. Res.*, *92*, 83, 1987.

Frank, L. A., W. R. Paterson, K. L. Ackerson, S. Kokubun, T. Yamamoto, D. H. Fairfield, and R. P. Lepping, Observations of plasmas associated with the magnetic signature of a plasmoid in the distant magnetotail, *Geophys. Res. Lett.*, *21*, 2967, 1994.

Fujimoto, M., and M. Nakamura, Acceleration of heavy ions in the magnetotail reconnection layer, *Geophys. Res. Lett.*, *21*, 2955, 1994.

Gosling, G. T., M. F. Thomsen, S. J. Bame, and C. T. Russell, Accelerated plasma flows at the near-tail magnetopause, *J. Geophys. Res.*, *91*, 3029, 1986.

Heyn, M. F., H. K. Biernat, R. P. Rijnbeek, and V. S. Semenov, The structure of reconnection layer, *J. Plasma Phys.*, *40*, 235, 1988.

Hones, E. W., Jr., Transient phenomena in the magnetotail and their relation to substorms, *Space Sci. Rev., 23*, 393, 1979.

Hudson, P. D., Rotational discontinuities in an anisotropic plasma, *Planet. Space Sci., 19*, 1693, 1971.

Hughes, W. J., and D. G. Sibeck, On the 3-dimensional structure of plasmoids, *Geophys. Res. Lett., 14*, 636, 1987.

Jeffrey, A., and T. Taniuti, *Non-Linear Wave Propagation*, Academic, San Diego, Calif., 1964.

Kantrowitz, A. R., and H. E. Petschek, MHD characteristics and shock waves, in *Plasma Physics in Theory and Application*, edited by W. B. Kunkel, p.148, McGraw-Hill, New York, 1966.

King, J. H., Interplanetary Medium Data Book-Appendix, *NSSDC/WDC-A-R&S Rep. 77-04a*, Sept. 1977.

Lee, L. C., and Z. F. Fu, A theory of magnetic flux transfer at the Earth's dayside magnetopause, *Geophys. Res. Lett., 12*, 105, 1985.

Lee, L. C., Y. Lin, Y. Shi, and B. T. Tsurutani, Slow shock characteristics as a function of distance from the *X*-line in the magnetotail, *Geophys. Res. Lett., 16*, 903, 1989.

Levy, R. H., H. E. Petschek, and G. L. Siscoe, Aerodynamic aspects of the magnetospheric flow, *AIAA J., 2*, 2065, 1964.

Lin, Y., and L. C. Lee, Chaos and ion heating in a slow shock, *Geophys. Res. Lett., 18*, 1615, 1991.

Lin, Y., and L. C. Lee, Structure of the dayside reconnection layer in resistive MHD and hybrid model, *J. Geophys. Res., 98*, 3919, 1993,

Lin, Y., and L. C. Lee, Structure of reconnection layers in the magnetosphere, *Space Sci. Rev., 65*, p.59, 1994a.

Lin, Y,. and L. C. Lee, Reconnection layer at the flank magnetopause in the presence of shear flow, *Geophys. Res. Lett., 21*, 855, 1994b.

Lin, Y., L. C. Lee, and C. F. Kennel, The role of intermediate shocks in magnetic reconnection, Res. *Geophys. Lett., 19*, 229, 1992.

Lui, A. T. Y., Characteristics of the cross-tail current in the Earth's magnetotail, in *Magnetospheric Currents*, Geophys. Monogr. Ser., Vol. 28, edited by T. A. Potemra, p. 158, AGU, Washington D. C., 1984.

Noshed, A., M. Scholar, T. Terasawa, S. J. Bame, G. Gloeckler, E. J. Smith, and R. D. Zwichl, Quasi-stagnant plasmoid in the middle tail: a new preexpansion phase phenomenon, *J. Geophys. Res., 91*, 4245, 1986.

Omidi, N. and D. Winske, Structure of slow magnetosonic shocks in low beta plasmas, *Geophys. Res. Lett., 16*, 907, 1989.

Petschek, H. E., Magnetic field annihilation, *in AAS-NASA Symposium on the Physics of Solar Flares, NASA Spec. Publ., SP-50*, 425-439, 1964.

Postman, G., G. Haerendel, I. Papamastorakis, N. Sckopke, S. J. Bame, J. T. Gosling, and C. T. Russell, Plasma and magnetic field characteristics of magnetic flux transfer events, *J. Geophys. Res., 87*, 2159, 1982.

Russell, C. T., and R. C. Elphic, Initial ISEE magnetometer results: Magnetopause observations, *Space Sci. Rev., 22*, 691, 1978.

Sato, T., Strong plasma acceleration by slow shocks resulting from magnetic reconnection, *J. Geophys. Res., 84*, 7177, 1979.

Schindler, K., Plasma and fields in the magnetospheric tail, *Space Sci. Rev., 17*, 589, 1975.

Scholar, M., Magnetic flux transfer at the magnetopause based on single *X* line bursty reconnection, *Geophys. Res. Lett., 15*, 291, 1988.

Scholar, M., D. N. Baker, S. J. Bame, W. Baumjohann, G. Gloeckler, F. M. Ipavich, E. J. Smith, and B. T. Tsurutani, Correlated observations of substorm effects in the near-earth region and deep magnetotail, *J. Geophys. Res., 90*, 4021, 1985.

Schwartz, S. J., M. F. Thomsen, W. C. Feldman, and F. T. Douglas, Electron dynamics and potential jump across slow mode shocks, *J. Geophys. Res., 92*, 3165, 1987.

Shi, Y. and L. C. Lee, Structure of the reconnection layer at the dayside magnetopause, *Planet. Space. Sci., 38*, 437, 1990.

Sibeck, D. G., G. L. Siscoe, J. A. Slavin, E. J. Smith, S. J. Bame, and F. L. Scarf, Magnetotail flux ropes, *Geophys. Res. Lett., 11*, 1090, 1984.

Smith, E. J., J. A. Slavin, B. T. Tsurutani, W. C. Feldman and S. J. Bame, Slow mode shocks in the Earth's magnetotail: ISEE-3, *Geophys. Res. Lett., 11*, 1054, 1984.

Sonnerup, B. U. O., G. Postman, I. Papamastorakis, N. Sckopke, G. Haerendel, S. J. Bame, J. R. Asbridge, J. T. Gosling and C. T. Russell, Evidence for magnetic reconnection at the Earth's magnetopause, *J. Geophys., Res., 86*, 10049, 1981.

Swift, D. W., On the structure of the magnetic slow switch-off shock, *J. Geophys. Res., 88*, 5685, 1983.

Swift, D. W., and L. C. Lee, Rotational discontinuities and the structure of the magnetopause, *J. Geophys. Res., 88*, 111, 1983.

Tsurutani, B. T., et al., Magnetic structure of the distant geotail from ~60 to ~220*Re*: ISEE-3, *Geophys. Res. Lett., 11*, 1, 1984.

Tsurutani, B. T., M. E. Burton, and E. J. Smith, Statistical properties of magnetic field fluctuations in the distant plasmasheet, *Planet. Space Sci., 35*, 289, 1987.

Ugai, M., Self-consistent development of fast magnetic reconnection with anomalous plasma resistivity, *Plasma Phys. Controlled. Fusion, 26*, 1549, 1984.

Vu, H. X., J. U. Brackbill, and D. Winske, Multiple switch-off slow shock solutions, *J. Geophys. Res., 97*, 13839, 1992.

Winske, D., and N. Omidi, Electromagnetic ion/ion cyclotron instability at slow shocks, *Geophys. Res. Lett., 17*, 2297, 1990.

Winske, D., E. K. Stover, and S. P. Gary, The structure and evolution of slow mode shocks, *Geophys. Res. Lett., 12*, 295, 1985.

Wu, C. C., and C. F. Kennel, Structure and evolution of time-dependent intermediate shocks, *Phys. Rev. Lett., 68*, 56, 1992.

Wu, B. H., J. K. Chao, W. H. Tsai, Y. Lin, and L. C. Lee, A hybrid simulation of contact discontinuity, *Geophys. Res. Lett., 21*, 2059, 1994.

Yamamoto, T., K. Shiokawa, and S. Kokubun, Magnetic field structures of the magnetotail as observed by GEOTAIL, *Geophys. Res. Lett., 21*, 2875, 1994.

Yan, M., L. C. Lee, and E. R. Priest, Fast magnetic reconnection with small shock angles, *J. Geophys. Res., 97*, 8277, 1992.

L. C. Lee, Geophysical Institute and Department of Physics, University of Alaska, Fairbanks, AK 99775-7320.

Y. Lin, Department of Physics, 206 Allison Lab, Auburn University, Auburn, AL 36849-5311. (e-mail: ylin@physics.auburn.edu)

(Received February 6, 1995; revised April 27, 1995;
accepted May 15, 1995.)